PERIODICO di MINERALOGIA
established in 1930

Dipartimento di Scienze della Terra
Sapienza Università di Roma

An International Journal of
Mineralogy, Crystallography, Geochemistry,
Ore Deposits, Petrology, Volcanology
and applied topics on Environment, Archaeometry and Cultural Heritage

In vitro toxicity of short vs long chrysotile fibres

Alessandro F. Gualtieri [1], Serena Mirata [2,3], Vanessa Almonti [3,4], Anna Maria Bassi [3,4], Chiara Meo [1], Sonia Scarfì [2,3,*], Mauro Zapparoli [5], Tatiana Armeni [6], Laura Cianfruglia [6], Daniela Marzioni [7], Sonia Fantone [7], Giovanni Tossetta [7], Pierluigi Stipa [8], Emiliano Laudadio [8], Simona Sabbatini [8], Cristina Minnelli [8], Silvia Di Valerio [9], Salvatore Vaiasicca [9], Antonio D. Procopio [9], Armanda Pugnaloni [9]

[1] Department of Chemical and Geological Sciences, University of Modena and Reggio Emilia, Modena, Italy
[2] Department of Earth, Environment and Life Sciences, University of Genova, Genova, Italy
[3] Inter-University Center for the Promotion of the 3Rs Principles in Teaching & Research (Centro 3R), Pisa, Italy
[4] Department Experimental Medicine, University of Genova, Genova, Italy
[5] Centro Interdipartimentale Grandi Strumenti (CIGS), University of Modena and Reggio Emilia, Modena, Italy
[6] Department of Odontostomatologic and Specialized Clinical Sciences, Polytechnic University of Marche, Ancona, Italy
[7] Department of Experimental and Clinical Medicine, Polytechnic University of Marche, Torrette di Ancona, Italy
[8] Department of Chemistry Division, Polytechnic University of Marche, Italy
[9] Department of Clinical and Molecular Sciences, Polytechnic University of Marche, Torrette di Ancona, Italy

ARTICLE INFO

Submitted: February 2023
Accepted: July 2023
Available on line: August 2023

* Corresponding author:
soniascarfi@unige.it

Doi: 10.13133/2239-1002/18012

How to cite this article:
Gualtieri A.F. et al. (2023)
Period. Mineral. 92, 203-222

ABSTRACT

Chrysotile is a natural hydrous layer silicate that belongs to the serpentine group. Because of its unique asbestiform shape and outstanding physical-chemical properties, chrysotile is still nowadays the most used commercial mineral fibre in the world. This occurs despite the mineral has been classified as a *Group 1* carcinogen by the International Agency for Research on Cancer (IARC). Since the "fibre toxicity paradigm" relies on the fibre size (length L and width W) and biodurability, the present work attempts to shed light on the issue of the toxicity of short vs. long chrysotile fibres by investigating two size-separated batches of chrysotile fibres (L>5 μm and L≤5 μm) of a commercial Russian sample. In parallel, UICC crocidolite and NYAD G wollastonite fibres were used as a positive and a negative carcinogenic standard, respectively. The calculated fibre potential toxicity/pathogenicity index (FPTI) value of the long-fibre chrysotile (2.35) is greater than that of the short-fibre (2.18) predicting a greater potential of toxicity/pathogenicity of the former. The FTPI value of short-fibre chrysotile is greater than that of wollastonite (1.92-2.12) but lower than that of crocidolite (2.67). The theoretical predictions were complemented with *in vitro* toxicity tests performed in parallel on four different cell types involved in the toxicity of inhaled mineral fibres: alveolar, endothelial, mesothelial cells and macrophages. The results from the MTT and LDH toxicity and ROS production tests are in line with the FPTI prediction. The negative carcinogenic standard wollastonite displays the lower *in vitro* toxicity score (0.25), while the short-fibre chrysotile presents a higher score (0.43), followed by the long-fibre chrysotile (0.66) and the positive carcinogenic standard crocidolite (0.67).
In conclusion, our *in vitro* acute toxicity results on chrysotile are in line with the FPTI model predictions, indicating that short chrysotile asbestos fibres should not be assimilated to "innocuous dusts".

Keywords: asbestos; mineral fibres; oxidative stress; carcinogenicity; predictive model.

BACKGROUND

Chrysotile, with ideal formula $Mg_3(OH)_4Si_2O_5$, is a natural hydrous layer silicate that belongs to the serpentine group. The structure is basically composed of one Mg-centred octahedral sheet covalently bonded to one Si-centred tetrahedral sheet (Ballirano et al., 2017). As already suspected by Pauling (1930), the three-dimensional crystal lattice of chrysotile is unique in nature. In fact, the size of an ideal octahedral sheet is greater than that of an ideal tetrahedral sheet. The misfit induces a differential stress that, to a first approximation, is released by rolling the layers into a cylindrical structure which provides chrysotile its peculiar fibrous habit (Baronnet and Devouard, 1996; Ballirano et al., 2017). Single rolled layers of chrysotile (fibrils) grow as aggregates to form fibre bundles with frayed ends and bending, distinctive of the asbestiform crystal habit. Because of its unique asbestiform shape and outstanding physical-chemical properties, chrysotile has been the most used commercial asbestos in the world and is still used today in the countries that have not banned it (Gualtieri, 2012).

In 2012, the IARC reported that there is enough scientific evidence that chrysotile together with five amphibole asbestos species should be classified as "carcinogenic to humans" (*Group 1*).

Being a carcinogen does not mean it cannot be used. Truth is that the majority of the countries worldwide still mine, manufacture and utilize chrysotile today allowing the so-called "safe use" (i.e., the use wearing individual protection devices to minimize exposure). This is possible because it is assumed that being not biodurable (the ability to persisting in the human body regardless of bio-chemical attack), chrysotile is less potent in the induction of lung cancer and malignant mesothelioma than amphibole asbestos (Bernstein et al., 2013). During the process of phagocytosis of a chrysotile fibre by alveolar macrophages in the lungs or pleural space, the acidic environment of the phagolysosomes degrades the chrysotile non-biodurable fibre, that undergoes dissolution with the leaching of Mg and production of amorphous silica relicts, subsequently eliminated by macrophages. Conversely, amphibole asbestos fibres are biodurable and prompt chronic inflammation responsible for adverse effects *in vivo* (Bernstein et al., 2013). The "fibre toxicity paradigm" is not universally accepted because it is an approximation that does not account for the role of many other parameters such as surface reactivity and the release of metals during the dissolution of the fibres (Gualtieri, 2023). The divisive situation has created two fronts: the "pro-chrysotile" side and the "ban-chrysotile" side. The latter considers all the regulated asbestos fibres, including chrysotile, toxic and carcinogenic and asks for their global ban (see Ramazzini Collegium, 1999).

As seen above, the "fibre toxicity paradigm" relies on the fibre dimensions and biodurability with health hazard represented by long, thin, and biodurable fibres. This hypothesis has a ground in the Stanton et al. (1981) observations that fibres with $L \leq 8$ μm and $W < 0.25$ μm are carcinogenic when implanted within the pleural cavity. Although Stanton et al. reported that smaller fibres were not necessarily innocuous in their model system, but rather induced tumours much less readily than long thin fibres (Goodglick and Kane, 1990), their findings certainly inspired the counting criteria of regulated fibres ($L \geq 5$ μm, $W < 3$ μm and $L/W > 3$) delivered by the World Health Organization (WHO). It is obvious that the "pro-chrysotile" side, relying on the "fibre toxicity paradigm" model, assumes that short non-biodurable chrysotile fibres do not actually represent a hazard to human health. The assumption that short chrysotile fibres are less or not hazardous with respect to the long ones is also strongly opposed and still open to debate.

The review of *in vitro*, *in vivo,* and epidemiologic data evidences contradictory results on the detrimental activity of short vs. long asbestos fibres, with a number of open issues. For example, there are currently no validated toxicological data to confirm that cleavage fragments with the dimensional criteria laid down by the WHO for "fibre" are less toxic than their asbestiform counterparts (ANSES, 2015; 2017). An early work by Bey and Harington (1971) reported no difference in the toxicity of long and short chrysotile or amosite fibres to peritoneal macrophages in the presence of serum. Goodglick and Kane (1990) claimed that both long and short crocidolite asbestos fibres are toxic to macrophages *in vitro* via an oxidant and iron-dependent mechanism while short fibres are cytotoxic *in vivo* when the clearance of these fibres is prevented. These authors also called for the very basic question "*are smaller fibres innately less harmful or are smaller fibres less injurious in vivo because they are cleared or sequestered more efficiently than larger fibres from sites of potential damage*?" Dodson et al. (2003) reviewed literature data and argued that asbestos fibres of all lengths induce pathological responses. According to Roggli (2015), the fact that short fibres cannot be ignored because they predominate in most samples can similarly be applied to non-fibrous particles in the lungs and thus has no merit in terms of asbestos causation. Boulanger et al. (2014) also leave the issue open reporting that exposure to longer fibres was associated with higher rates of lung cancer, but no definitive conclusion can be ascertained for the other size classes. Nevertheless, the authors noted that exposure to short, thin fibres was associated with lung cancer risk.

In support of the thesis that short fibres are more hazardous than long fibres, Yeager et al. (1983) reported

that a natural short chrysotile fibre was more toxic to human alveolar macrophages than UICC raw chrysotile. Egilman (2009) stated that several studies (see for example, LeBouffaunt et al., 1974) on pleural fibres found short chrysotile as the only fibre type observed and almost always the predominant fibre in patients with mesothelioma. Among these studies, Suzuki et al. (2005) claimed that short, thin, asbestos fibres contribute to the causation of human malignant mesothelioma and that it is not prudent to take the position that short asbestos fibres convey little risk of disease. It should be remarked that later Roggli (2015) evidenced numerous problems with the experimental results of the work by Suzuki et al. (2005).

The hypothesis that long fibres are more hazardous than short fibres, with special attention to chrysotile, is recognized by Kaw et al. (1982) who reported that longer chrysotile, crocidolite, and amosite fibres were slightly more toxic to peritoneal macrophages in the presence of serum than were an equal mass of corresponding short fibres. Hesterberg and Barrett (1984) found that milled (shorter) chrysotile was less effective than raw (longer) chrysotile in inhibiting the proliferation and morphological transformation of Syrian hamster embryo cells. Davis and Jones (1988) found no convincing evidence for pathogenicity of amphibole and chrysotile fibres ≤5 μm in length. According to Riganti et al. (2003), short amphibole asbestos amosite fibres, obtained by grinding longer ones, exhibited a lower potential to damage nude DNA and a lower *in vitro* cytotoxicity. In 2004, the Agency for Toxic Substances and Disease Registry published that: "*Given findings from epidemiologic studies, laboratory animal studies, and in vitro genotoxicity studies, combined with the lung's ability to clear short fibres, (expert) panelists agreed that there is a strong weight of evidence that asbestos and SVFs shorter than 5 μm are unlikely to cause cancer in humans*" (ATSDR, 2004). In his review, Roggli (2015) concludes that inhalation studies in animal models have demonstrated that fibres >5 μm in length are associated with asbestosis, mesothelioma and lung cancer, with no convincing evidence for a pathogenic effect for fibres ≤5 μm in length. Similarly, *in vitro* studies do not override inhalational studies of whole animals or the epidemiological findings in humans. Barlow et al. (2017) concluded that studies reported over the last several decades have consistently supported the conclusion that there is very little if any risk in humans associated with exposure to fibres <5 μm. Bernstein (2022) also concluded that "*epidemiology, toxicology, and in vitro studies provide strong support that short chrysotile and amphibole asbestos fibres with lengths <5-10 μm do not contribute to the health effects of asbestos. The epidemiology studies in which the cancer potency estimates were based upon relatively high exposure concentrations provide a conservative assessment that shorter fibres would have little if any effect*". These findings are also supported by a statistical evaluation of various criteria for carcinogenic potency in the scientific literature made by Korchevskiy and Wylie (2022) who found that the Stanton criteria were a relevant predictor of the carcinogenic potency of elongate mineral particles. Bernstein (2022) finally claimed that chrysotile present in the brake dust is largely smaller than 5 μm showing no significant pathological response in the respiratory tract compared to the air control group.

In the attempt to shed light on the issue of the toxicity of short vs. long chrysotile fibres, this work reports the results of a comparative *in vitro* toxicity study of two batches of chrysotile fibres with L>5 μm and L≤5 μm separated by cryogenic milling from a commercial Russian sample. To test the accuracy of the experimental procedures a UICC crocidolite sample has been used as positive carcinogenic standard and NYAD G wollastonite has been used as negative carcinogenic standard.

MATERIALS AND METHODS

All reagents were acquired from SIGMA-ALDRICH (Milan, Italy), unless otherwise stated.

The mineral fibres

Chrysotile fibres used in this study were separated from a commercial sample produced by the Orenburg Minerals mine near Yasny (in Russian "Я́сный"=clear and sometimes found in the maps as Yasnij, Yasniy, Yasnyj or Yuzhnyi), in the Orenburg region, southern Ural Mountains (Russia). The chrysotile fibres were identified as clinochrysotile with minor orthochrysotile, displaying the mean chemical formula $(Mg_{2.870}Fe^{2+}_{0.027}Al_{0.034}Cr_{0.005}Ni_{0.006})_{2.986}(OH)_4Si_{1.92}O_5$ and a measured density of 2.578(2) g/cm^3 (Di Giuseppe et al., 2021a). The full crystal-chemical characterization of the sample can be found in Di Giuseppe et al. (2021a). A selection of the fibres under the optical microscope was accomplished to obtain high purity batches for the *in vitro* tests. We cannot rule out that a very minor mineral impurities associated with chrysotile in the pristine sample, namely lizardite-1T, magnetite, hydromagnesite and calcite, were retained in the separated batches.

Crocidolite has been selected for this study as positive carcinogenic standard as it is classified by the IARC in Group 1 "Carcinogen for humans" (IARC, 2012). The used UICC standard crocidolite (South African, NB #4173-111-3) has mean chemical formula of $(Na_{1.96}Ca_{0.03}K_{0.01})_2(Fe^{2+}_{2.34}Fe^{3+}_{2.05}Mg_{0.52})_{4.91}(Si_{7.84}Al_{0.02})_{7.86}O_{21.4}(OH)_{2.64}$. The sample contains minor (<1 wt%) impurities of hematite, magnetite, and quartz. The measured mean

L and W of the fibres are 18(1) μm and 0.35(1) μm, respectively. The density of the sample is 3.35 g/cm^3 and the surface specific area (SSA) is 16.1(8) m^2/g (Gualtieri et al., 2018).

Wollastonite has been selected as negative carcinogenic standard. The used NYAD G wollastonite mainly contains wollastonite-1A and minor calcite. It has a mean chemical formula of $Ca_{0.997}Fe^{2+}_{0.0053}Fe^{3+}_{0.0024}Mn_{0.0025}Mg_{0.0009}Si_{0.9786}O_3$, a measured mean L and W of the fibres of 46.6 μm and 3.74 μm, respectively, a density of 2.980(3) g/cm^3 and SSA = 0.50(1) m^2/g (Di Giuseppe et al., 2021b).

The size separation of the chrysotile fibres

We used a Retsch mixer mill MM 400 (Düsseldorf, Germany) for the cryogenic milling of the chrysotile fibres and size separation. A detailed description of the procedure is found in Scognamiglio et al. (2021). The milling jars (35 mL) are made of steel and contain a steel milling ball while the lining of the jar and balls is made of polytetrafluoroethylene (PTFE) to prevent contamination of the sample with metals from the jar and balls during milling. For the cryogenic milling, the jar is submerged in liquid nitrogen (cryogenic conditions) and subsequently mounted in the mixer mill. During operation, the jar oscillates with a pre-set frequency (3–30 Hz). Short chrysotile fibres (95% L≤5 μm) were obtained by cryogenic milling for 40 min while a milling time of 5 min was sufficient to yield a sample mainly composed of long chrysotile fibres (90% L>5 μm). For the short (≤5 μm) chrysotile fibres, we measured a mean L of 1.91(0.21) μm (Scognamiglio et al., 2021), a mean W of 0.15(7) μm and SSA of 30.3(1.0) SSA m^2/g. For the fraction of long (>5 μm) chrysotile fibres, we measured a mean L of 29.80(3.08) μm (Scognamiglio et al., 2021), a mean W of 0.4(1) μm and SSA of 28.9(1.2) m^2/g.

The FPTI model for the determination of the potential toxicity of the samples

The values of FPTI of the samples with long and short chrysotile fibres were calculated according to the method described in Gualtieri et al. (2018). The FPTI model is a theoretical tool predicting the potential toxicity and carcinogenicity of a mineral fibre based on all its morphometric, chemical, biodurability and surface parameters inducing biological adverse effects. These effects may determine the cyto-toxicity and geno-toxicity *in vitro* (acute effects in cell cultures), cyto-toxicity and geno-toxicity *in vivo* (acute and medium-term effects in animal studies, namely rats), and pathogenicity (carcinogenicity) *in vivo* (long term-chronic effects in animals and human epidemiological studies). Table 1 summarises the model parameters used to calculate the FPTI of the chrysotile samples considered in this study. For each parameter, a score is assigned depending on its measured value and its supposed susceptibility in inducing adverse effects. The sum of the scores gives the value of the FPTI associated with the mineral fibre (Table 1). It must be remarked that the measured value of each parameter identifies a class (column 2 in Table 1) and consequently a normalized score of the model (column 3 in Table 1). An error is associated to a normalized score and its calculation has been recently revised and described in detail in the manual of the software available at the Web-FPTI site fibers.unimore.it/?page_id=972. Further information regarding the calculation of scores and the FPTI index can be found in Gualtieri (2018) and Mossman and Gualtieri (2020).

In vitro cytotoxicity tests

The cytotoxic effect of the mineral fibres with the MTT test was assessed using four cell lines. The MTT test (Ciapetti et al., 1993) measures the mitochondrial enzyme activity by quantifying resultant alterations of energy metabolism and, therefore, cell toxicity. Fibre suspensions were prepared with 50 μg/ml of each previously autoclaved material (14 μg/cm^2) per ml of culture medium. In preliminary experiments different fibre resuspension procedures were tried: vortexing at maximum speed (40 Hz) for 1 min or sonicating (50 Hz alternate pulses of 1-2 sec) for 5 min at 0 °C. The latter was then chosen as the final fibre preparation procedure for all the experiments obtaining the optimal fibre dispersion in aqueous solution. 50 μg/ml was the selected concentration that produces well-defined cell responses to compare the mineral cytotoxic action and their effects on cells at experimental points.

In the tests with the HECV endotheliocytes and in THP-1-derived M0 macrophages, HECV cells were plated in quadruplicate at 10,000 cells/well in 96-well plates, while THP-1 cells were seeded in quadruplicate at 50,000 cells/well in 96-well plates and differentiated to M0 macrophages with 20 ng/mL PMA for 48 h. After fresh medium substitution, the mineral fibres were added to each well at a final concentration of 50 μg/mL, and the plates were incubated for 24 h or for 48 h before cell viability was evaluated by the MTT assay (0.5 mg/mL final concentration) as described in Mirata et al. (2022). The absorbance was read at 540 nm in a plate reader (BMG Labtech, Ortenberg, Germany). Data are the means ±SD of three independent experiments performed in quadruplicate.

In the other cellular tests, other two cell lines were used: Human cell lines MeT5A (SV40-immortalized pleural mesothelial cells) and A549 consisting of hypotriploid alveolar basal epithelial cells. The latter was first developed

Table 1. The parameters of the FPTI model with the values calculated for the raw chrysotile from Russia (Di Giuseppe et al., 2021), the same chrysotile with L >5 μm and with L≤5 μm (both in this work).

Parameters	Classes	Normalized score $FPTI_i$	Russian chrysotile	Russian chrysotile >5 mm	Russian chrysotile ≤5 mm
(1.1) length L	>5mm and ≤10mm	0.100	0.400	0.400	0.000
	>10mm and ≤20mm	0.200			
	>20mm	0.400			
(1.2) diameter D	>1mm and ≤3mm	0.100	0.200	0.200	0.400
	>0.25mm and ≤1mm	0.200			
	≤0.25mm	0.400			
(1.3) crystal curvature	Flat surface (perfect crystal)	0.050	0.200	0.200	0.200
	Altered surface	0.100			
	Cylindrical surface	0.200			
(1.4) crystal habit	Curled	0.100	0.100	0.100	0.100
	Mixed Curled/acicular	0.200			
	Acicular	0.400			
(1.5) fibre density	≤2.75 g/cm^3	0.050	0.050	0.050	0.050
	>2.75 and ≤3.5 g/cm^3	0.100			
	>3.5 g/cm^3	0.200			
(1.6) hydrophobic character of the surface	Hydrophobic	0.050	0.200	0.200	0.200
	Amphiphilic	0.100			
	hydrophilic	0.200			
(1.7) surface area	>25 m^2/g	0.050	0.100	0.050	0.050
	≤25 and >5 m^2/g	0.100			
	≤5 m^2/g	0.200			
(1.8) Total iron content	Fe_2O_3+FeO wt% <1	0.050	0.100	0.100	0.100
	1≤ Fe_2O_3+FeO wt% ≤10	0.100			
	Fe_2O_3+FeO wt% >10	0.200			
(1.9) ferrous iron	0 ≤ FeO wt% ≤0.25	0.050	0.100	0.100	0.100
	0.25 < FeO wt% ≤1	0.100			
	FeO wt% >1	0.200			
(1.10) Surface ferrous iron/iron nuclearity	Fe^{2+} nuclearity >2	0.020	0.030	0.030	0.030
	Fe^{2+} nuclearity =2	0.030			
	Fe^{2+} nuclearity =1	0.070			
(1.11) content of metals other than iron*	$\sum_i \frac{C_i}{L_i} \leq 1$	0.100	0.400	0.400	0.400
	$1 < \sum_i \frac{C_i}{L_i} \leq 5$	0.200			
	$\sum_i \frac{C_i}{L_i} > 5$	0.400			
(1.12) dissolution rate log(R)**	≤1y	0.050	0.050	0.050	0.050
	>1 and ≤40y	0.100			
	>40y	0.200			
(1.13) velocity of iron release***	≤0.1	0.033	0.133	0.133	0.133
	>0.1 and ≤1	0.067			
	>1	0.133			
(1.14) velocity of silica dissolution****	<0.5	0.016	0.067	0.067	0.067
	>0.5 and <1	0.033			
	>1	0.067			

Table 1. ... Continued

Parameters	Classes	Normalized score $FPTI_i$	Russian chrysotile	Russian chrysotile >5 mm	Russian chrysotile ≤5 mm
(1.15) velocity of release of metals*****	<1	0.033	0.133	0.133	0.133
	>1 and <10	0.067			
	>10	0.133			
(1.16) z potential	Negative at pH=4.5	0.100	0.100	0.100	0.100
	Negative at both pH=4.5 and 7	0.200			
(1.17) fibres' aggregation	V>|20|	0.033	0.033	0.033	0.067
	|10|<V<|20|	0.067			
	|0|<V<|10|	0.133			
(1.18) Cation exchange (in zeolites)	cation Exchange	0.067	0.000	0.000	0.000
	no cation exchange	0.000			
		FPTI (error§)	2.40(0.07)	2.35(0.05)	2.18(0.07)

* $\sum_i \frac{C_i}{L_i}$ = sum of the concentrations of heavy metals (Sb, As, Hg, Cd, Co, Cr, Cu, Pb, Ni, Zn, V, Be) C_i in the fibre (ppm) divided by the limit L_i for that metal according to the existing regulatory system except for Be with limit = 0.5 ppm; ** the total dissolution time of the fibre calculated in years (y) following the standardized acellular *in vitro* dissolution model at pH=4.5 described in reference (Gualtieri et al., 2018); *** total content of elemental iron in the fibre (wt%) possibly made available as active iron at the surface of the fibre divided by the total dissolution time (y) of the fibre (y); **** total content of Si of the fibre (wt%) divided by the total dissolution time (y) of the fibre; ***** total content (ppm) of heavy metals (Sb, As, Hg, Cd, Co, Cr, Cu, Pb, Ni, Zn, V, Be; Mn, Be) divided by the total dissolution time (y) of the fibre; § the calculated error takes into account how close it is the value of the fibre parameter to the neighbour class. For the threshold values, the error is the half of the variation (Δ) between adjacent FPTI scores. The error varies with the distance from the threshold values following a law of exponential decay $(\Delta/2)/e^{s}$ with Δ=half of the variation between adjacent FPTI scores; s=step between the values of the parameters. For example, if the measured value of the mean fibre length L is =10 μm, the error associated to the FPTI score of the fibre length L parameter is 0.05. This number is half of the difference values between the class of FPTI 0.1 and 0.2 (0.2-0.1=0.1; 0.1/2=0.05). Error decreases following the exponential decay above with the distance from the threshold value (10 μm). If the measured value of the mean fibre length L=13 μm, the error associated to the FPTI score of the fibre length L parameter is 0.002489, that is $[(0.05)/2]/e^{(13-10)}$. The qualitative parameters (1,3), (1,4), (1,6), (1,16), and (1,18) has an associated Error=0.

by removing and culturing pulmonary carcinoma tissue from the explanted tumor of a 58-year-old Caucasian male. The A549 cells are usually used to model the alveolar Type II pulmonary epithelium monolayer in vitro. Both cell lines were grown in controlled atmosphere in RPMI-164 supplemented with 10% fetal bovine serum (both from Gibco, USA), 2 mM l-glutamine, 100 U/ml penicillin and 100 U/ml streptomycin (Sigma-Aldrich, Milano, Italy). Cells were passaged every 1-3 days by digestion with 0.25% trypsin (Sigma-Aldrich) containing 0.02% EDTA. After seeding, cells were left to adhere to the substrates for 24 h. The spent culture medium was then replaced with the mineral suspensions. Cells were left in contact with mineral suspensions for 24 and 48h. Untreated cultures were considered as control samples (ctr). For MTT assay MeT5A and A549 cells were seeded at a density of 3×10^4 cells/well into 24-well microplates in three replicates. After treatment, the medium was removed and 200 µl MTT solution (Sigma, St. Louis, USA. 5 mg/ml in RPM1-1640) and 1.8 ml RPM1-1640 were added to cells. The multiwell plates were then incubated at 37 °C for 3 h. After discarding supernatants, the formazan crystals were dissolved in 2 ml of solvent (4% HCl, 1 M in absolute isopropanol). The amount of formazan crystals is directly related to the number of viable cells. Optical density (OD) was read at 540 nm using a spectrophotometer (Neo Biotech NB-12-0035). Untreated cells were used as controls and their absorbance values taken as reference. Results were expressed as mean ± standard deviation (sd) of % values of viable cells. Control monolayers were grown in culture medium with no treatments; their absorbance values were taken as reference values and considered as 100% of cell viability. Data obtained from three assays were expressed as mean values ± standard deviation.

Light microscopy investigations

Morphological investigations of mineral treated cultures were performed at 24 and 48 h by Nikon Eclipse Ti inverted light microscope fitted with a Nikon DS-L2 camera control. Images were collected at 20´ original magnification.

Plasma Membrane Damage by LDH Assay

The plasma membrane disturbance caused by the mineral fibres was evaluated with the LDH assay, which measures the intracellular LDH released in the media by damaged cells through the quantification of its enzymatic activity. Briefly, THP-1 cells and HECV cells were seeded in quadruplicate on 96-well plates, and the experiment was performed as described for the MTT assay. After 24 h or 48 h of exposure to the mineral fibres, the LDH release in the cell media was assessed by transferring 100 µL of cell medium from each well into a new plate and adding 100 µL of assay buffer (686 µM iodonitrotetrazolium chloride, 291 µM 1-methoxyphenazine methosulphate, 1.35 mM µ-NAD and 55.5 mM lithium L-lactate in 200 mM TRIS, pH 8.2). Then, the plate was incubated at room temperature for 30 min, the reaction was blocked with 50 µL of 1 M acetic acid and the absorbance was read at 490 nm in a plate reader (BMG Labtech, Ortenberg, Germany). A positive control of 100% lysed cells was also obtained by adding 0.1% Triton X-100 to the wells of untreated cells and incubating for 10 min at 37 °C before adding the LDH assay buffer. Data are the means ±SD of three independent experiments performed in quadruplicate.

Reactive Oxygen Species (ROS) Production in THP-1 and HECV cells

To evaluate the intracellular production of ROS induced by the mineral fibres, THP-1 cells and HECV cells were seeded in 96-well plates at the same concentrations reported for the MTT assay. Then, after being washed once with Hank's Balanced Salt Solution (HBSS), cells were incubated for 45 min at 37 °C with 10 µM 2',7' -dichlorodihydrofluorescein diacetate dye in HBSS (Life Technologies) and washed with HBSS to remove excess dye. Intracellular ROS production was measured after cells were treated with 50 µg/mL of mineral fibres added to the cells in complete RPMI medium (without phenol red giving its interference in the following fluorescence measurements) for 6 and 24 h at 37 °C, whereas a positive control with 200 and 500 µM H_2O_2 was prepared as well. Then, the plates were read on a FLUOstar® Omega multi-mode microplate reader (BMG Labtech) with 485/520 excitation/emission wavelengths. Data are the means ± SD of two independent experiments, in which each condition was tested eight times.

ROS production in MeT5A and A549 cells

Cellular oxidative stress induced by asbestos fibres treatments was measured using the fluorescent probe, H2DCFDA (Carboxy-H2DCFDA-C400, Invitrogen). The H2DCFDA crossing the plasma membrane of the cells is deacetylated to H2DCF producing a fluorescent product, DCF. MeT5A and A549 cells (1.5×10^4 and 1.0×10^4 cells/cm^2 respectively in 12-well plates) were seeded for 24 h in RPMI-1640 before treatments with asbestos fibres for 6 and 24h. 250 mM H_2O_2 treatment for 15 min in ice was used as positive control. At the end of each time points cells were trypsinized, centrifuged at 500 g for 7 min, washed twice with PBS (Phosphate Buffered Saline) (Euroclone). The cells were then incubated with PBS containing 10 µM (work solution) of Carboxy-H2DCFDA (1mM) probe for 30 min at 37 °C in the dark. After the incubation the reaction was stopped with 1ml of filtered PBS followed by centrifuged at 500 g for 7 min. The supernatant was then removed, and the cells resuspended in 200µl of filtered PBS. The cells were stained with 4µl of Propidium Iodide (PI) 10µg/ml to exclude dead cells from the counts. Fluorescence intensity was measured using flow cytometry (Guava® easy Cyte™ Flow Cytometer; Millipore) with excitation at 488 nm. To assess the intracellular ROS levels, cells were selected using standard morphological parameters (forward and side scattering). Emissions were recorded using the green channel for Carboxy-H2DCFDA and the red channel for the PI. Mean Fluorescence Intensity (MFI) was recorded on an average of 10,000 events from each sample. Experiments were carried out at least in triplicates and results were analysed by FlowJo software. Results were expressed as mean values ± standard deviation (sd) of fluorescence intensity.

Cellular Glutathione investigation (total GSH) at 24 h

Total glutathione was measured spectrophotometrically at 412 nm using the glutathione reductase (GR) recycling assay in the presence of 5,5-dithiobis (2-nitrobenzoic acid) (DTNB), with a calibration curve obtained with known concentrations of GSH. Briefly, the cells were trypsinized, washed twice in cold PBS, and deproteinized in 1% sulfosalicylic acid for 30 min at 4 °C. After centrifugation, the supernatant was recovered and analysed for glutathione quantification. The pellet was resuspended with 1 M NaOH for recovery and quantification of proteins by Bradford method using BSA as standard. Data are the mean ±SD of three independent experiment for each condition.

EPR spectra, Molar concentration of [DMPO HO] adduct

Fibres were suspended and incubated in 0.1 M H_2O_2 solution, buffered at pH 7.4, for 1 h, under stirring at room temperature. These conditions were chosen to promote the dissolution dynamics of asbestos in a reasonable experimental time mimicking the cellular environment. To assess the surface reactivity of the investigated systems, the system was induced to produce hydroxyl radicals (HO•) (Janzen, 1971; Buettner, 1987; Stipa, 2021) by the Fenton reaction: $Fe^{2+}_{surf} + H_2O_2 \rightarrow Fe^{3+}_{surf} + OH^- + OH\bullet$.

In the presence of the molecule 5,5-dimethyl-1-pyrroline N-oxide (DMPO) as Spin Trap, the surface-generated HO• radicals were rapidly trapped to yield the corresponding [DMPO-HO]• adduct, characterised by a typical EPR signal with four peaks. Each resulting recorded EPR spectrum was transformed by double integration to evaluate the total molar concentration of [DMPO-HO]• radicals released during 1 h of incubation of the asbestos fibres.

X-band EPR measurements have been carried out on a Bruker EMX/Xenon spectrometer system equipped with a microwave frequency counter and a Nuclear Magnetic Resonance (NMR) Gauss meter for field calibration. To determine the g-factor, the whole system was standardized with a sample of perylene radical cation in concentrated sulfuric acid, with a resulting value of 2.00258. Quantitative estimations were performed using the native (Xenon) spectrometer software, which was standardized with proper alanine samples. For the data acquisition, the instrument parameters were set up as follows: Modulation Frequency: 100 kHz; Time Constant: 0.01 ms; Sweep Width: 100 G; Modulation Power: 10.52 mW; Modulation Amplitude: 1.0 G; Sweep Time: 5.24 s.

RESULTS AND DISCUSSION

The FPTI classification

The values of FPTI of the samples with long and short chrysotile fibres calculated according to the method described in Gualtieri et al. (2018) are reported in Table 1 and show differences among the chrysotile samples. Indicatively, pristine Russian chrysotile and long-fibre Russian chrysotile display close FPTI values (2.40 and 2.35, respectively) while the short-fibre Russian chrysotile has a FPTI value of 2.18. The calculated FTPI values of the negative carcinogenic standard NYAD G wollastonite are 1.92(0.30) and 2.12(0.18) (Gualtieri, 2018; Di Giuseppe et al., 2021b) while the calculated FTPI value of the positive carcinogenic standard UICC crocidolite is 2.67(0.11) (Gualtieri, 2018). Among the parameters measured for the calculation of the FPTI index, most of them are identical for the three samples (i.e., crystal habit, surface hydrophobicity, total and ferrous iron content, content of metals, dissolution rate, velocity of release of metals and zeta potential). Only length (1,1), diameter (1,2), surface area (1,7) and (1,17) fibres' aggregation change. Finely ground Russian chrysotile is assigned a score of zero for the parameter (1,1) because the mean fibre L is below the threshold value of 5 μm. The other two chrysotile samples have a maximum score (0.40) for the parameter (1,1) as their mean fibre L values exceed the threshold value of 20 μm. On the other hand, the smaller mean diameter of the finely ground Russian chrysotile increases the FPTI normalized parameter from 0.2 to 0.4. Concerning the parameter (1,7), the raw chrysotile has the lowest value of SSA (18.4 m^2g^{-1}) compared to the other samples. The short and long chrysotile fibres have SSA values of 30.3 m^2g^{-1} and 28.9 m^2g^{-1}, respectively. As highlighted in our previous work, raw Russian chrysotile is a coarse material characterised by fibres aggregated into large bundles giving a small overall SSA. As expected, the reduction in fibre size induced by cryo-milling led to an increase in the SSA of the Russian chrysotile. The zeta potential driven fibres' aggregation is also slightly different in the finely ground Russian chrysotile.

In vitro assays

The MTT assay has been employed to measure the cell viability in four different human cell lines (THP-1-derived M0 macrophages, HECV endothelial cells, Met5A pleural mesothelial cells and A549 alveolar basal epithelial cells) treated with mineral fibres at a final concentration of 50 μg/ml for 24 h and 48 h. These data invariably evidenced a greater cytotoxic activity of the long chrysotile fibres compared to the short ones (chr grey columns in Figure 1a and 1b). The MTT tests also showed that the positive carcinogenic standard UICC crocidolite (cro red columns in Figure 1a and 1b) has a cytotoxic action at both 24 h and 48 h slightly lower or comparable to that of the chrysotile fibres. Conversely, at both time points, the negative carcinogenic standard NYAD G wollastonite (wol) is the less cytotoxic investigated fibre (white bars in Figure 1 a,b).

Images obtained from light microscopy investigations, plotted in Figure 2, showed aspects of cell perturbation in both treated MeT5A and in A549 cells with not significant time-dependent evidence with respect to the control cultures. 48h time points allow to better evaluate the structural cell alterations and culture densities. High levels of cell vacuolization were observed in both cell lines after the contact with the longer chrysotile fiber (chr>5) compared to the other treatments (chr≤5, cro) progressing to cell necrosis. After contact with wol, cells show less morpho-structural aspects of cell damage which appear to parallel the perturbation of cell viability evidenced by MTT assays.

Figure 3 reports the results of the LDH assay, which measures the level of plasma membrane damage induced in THP-1 M0 macrophages and in HECV endotheliocytes exposed for 24 h and 48 h to the fibres and generally reflect the level of cell death by a direct toxic effect. These data confirm the outcome of the MTT tests highlighting a greater direct cytotoxic activity of the long chrysotile fibres compared to the short ones (chr light grey vs dark grey columns, respectively, in Figure 3 a,b) and to crocidolite (cro red columns in Figure 3 a,b). Specifically, in THP-1 M0 macrophages at both time points neither

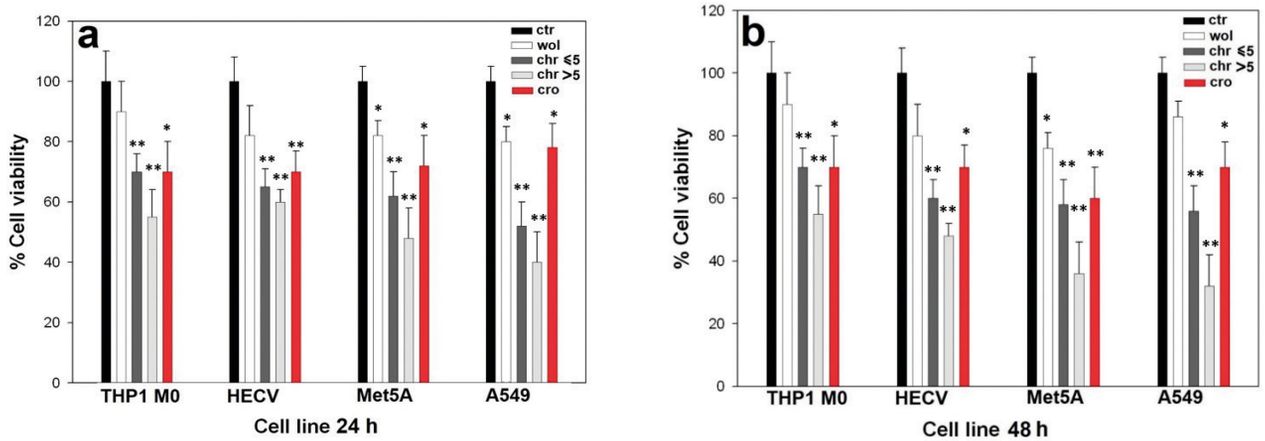

Figure 1. Plots of the results of the MTT cytotoxicity test using THP1, HECV, Met5A and A549 cell cultures at 50 mg/ml fibre concentration. (a) after 24 h. (b) after 48 h. Legend: ctr = control (black bars); wol = NYAD G wollastonite (white); chr≤5=Russian short (≤5 mm) chrysotile fibres (dark grey); chr>5=Russian long (>5 mm) chrysotile fibres (light grey); cro=UICC crocidolite (red). Asterisks indicate significance in Tukey paired test as compared to the relative untreated control (*p<0.05, **p<0.005, respectively).

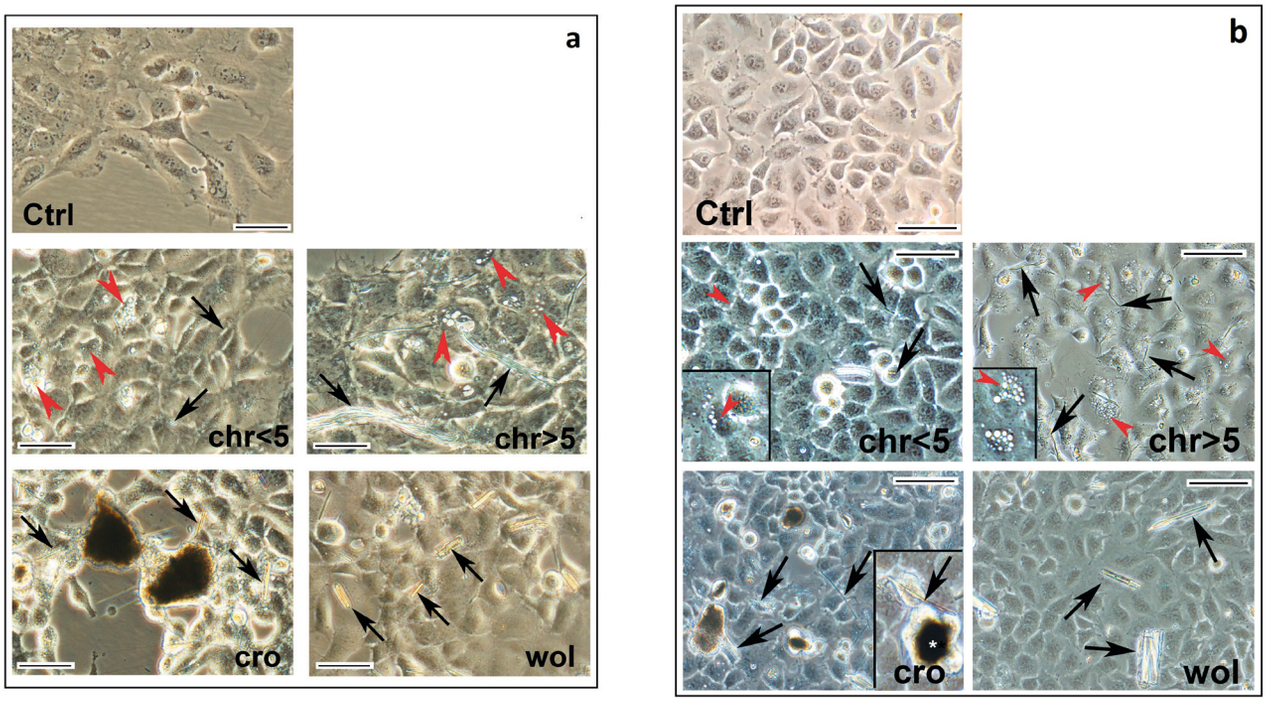

Figure 2. Light microscopy investigations of MeT5A mesothelial cells and A549 alveolar cells at 48 h in the presence of fibres (black arrows). Images obtained from bright field microscopy acquisition showed aspects of cell perturbation in both treated MeT5A and in A549 cells. Structural cell alterations were detected from 24 h time point with peculiar differences. High levels of cell vacuolization (red arrowhead) were observed in both cell lines after the contact with chrysotile fibres, more evident with the chrysotile longer fibres (chr>5) as compared to the other treatments (i.e., chr≤5, cro). After contact with the wol fibres, cells showed less morpho-structural aspects of cell damage. 20′ original magnification. Fig. 2b inserts, intracellular vacuoles in chr≤5 and chr>5 treated cells; clusters of cell debris (*) in cro treated cultures. Legend: ctr= control; wol= NYAD G wollastonite; chr≤5=Russian short (≤5 μm) chrysotile fibres; chr>5=Russian long (>5 μm) chrysotile fibres; cro=UICC crocidolite. The black bar approximately spans 20 μm.

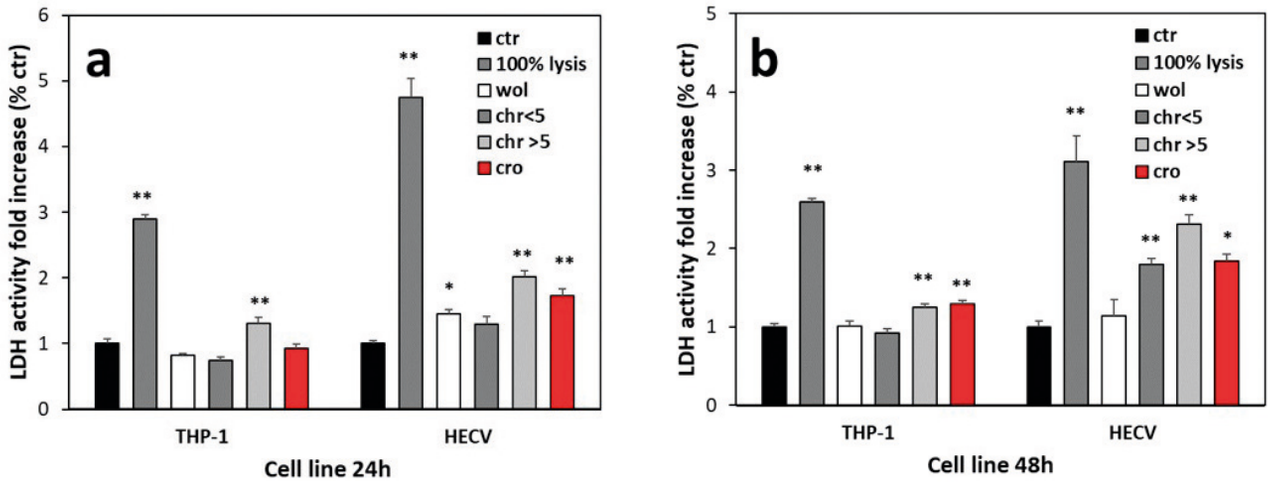

Figure 3. Plots of the results of the LDH cell membrane damage test using THP1 and HECV cell cultures, with fibre concentration at 50 mg/ml. (a) after 24 h. (b) after 48 h. Legend: ctr= control (black bars); 100% lysis= positive control lysed cells (dark grey); wol= NYAD G wollastonite (white); chr≤5=Russian short (≤5 μm) chrysotile fibres (dark grey); chr>5=Russian long (>5 μm) chrysotile fibres (light grey); cro=UICC crocidolite (red).

wollastonite nor the short-fibre chrysotile showed any substantial increase of LDH release, while crocidolite elicited a significant release mainly at 48 h (1.3-folds vs. ctr). Conversely, at both time points a significant leakage of the enzyme from macrophages is measured after long-fibre chrysotile treatment (~1.3-folds vs ctr), indicating that in this cell type a direct cytotoxic effect is mainly exerted by long chrysotile fibres. The same test in HECV endotheliocytes highlighted a slightly different behaviour. In particular, wollastonite only showed a direct membrane damage by LDH leakage at 24 h treatment (1.45-folds vs ctr), returning to the values of the control at 48 h, while crocidolite and the long-fibre chrysotile showed a significant LDH leakage at both time points, close or up to doubling the value of the control. Conversely, the short-fibre chrysotile LDH values showed a significant enzyme leakage only at 48 h (1.8-folds vs ctr, respectively). These results again indicate a higher direct cytotoxic potential of the long fibres as compared to the short ones and also a higher direct damaging effect of the fibres on endothelial cells as compared to immune cells. This suggests that the significant cytotoxicity of the chrysotile fibres measured by the MTT assay in macrophages is the sum of various cell death mechanisms, like for example apoptosis, other than the direct membrane damage highlighted by the LDH assay.

As far as the ROS production is concerned, the DCF test with THP1 cells at 6 h evidences a greater activity for the long chrysotile fibres as compared to the short ones (chr light vs dark grey columns in Figure 4a). A significant ROS production by the H_2O_2 positive control is also evident, at this time point. Conversely, at 6 h HECV cells show a lower ROS production upon all fibre treatment as compared to THP1-M0, although still significant respect to control cells. No difference between long and short chr fibre is observed. At 24 h (Figure 4b), both HECV and THP1-M0 cells show a higher ROS production in all fibre-treated samples as compared to the same treatments at 6 h, with no differences between short and long chr fibres, and with THP1 macrophages measuring the highest responses in terms of oxidative stress induction. This is likely a consequence of the phagocytosis process activated in these cells upon fibre contact, ROS in fact are usually produced to facilitate the foreign body dissolution inside the cells. The increased ROS production is also confirmed in Met5A and A549 cells after longer times of incubation (6 h and 24 h, Figure 4 c,d, respectively) where the ROS production from crocidolite (cro red columns in Figure 4 a,b) is also pronounced.

Figure 5 reports the results of the test of the oxidative state of Met5A and A549 cells after 24 h by measuring the decrease in reduced glutathione (GSH), which prolonged depletion is also considered an early hallmark of the progression of apoptosis (Circu and Aw, 2008). Although the data are scattered, once again the reduction is evident for all the investigated fibres in the MeT5A cells and mainly for the long chrysotile fibres (chr light grey columns), wollastonite (wol white columns) and crocidolite (cro red columns) in the A549 culture. These data confirm that the high oxidative state of the cells is maintained even after 24 h of fibre interaction, probably signalling the onset of apoptotic mechanisms in the stressed cells.

Figure 6 reports the release of free radicals in presence of H_2O_2 from wollastonite (a), short chrysotile fibres (b),

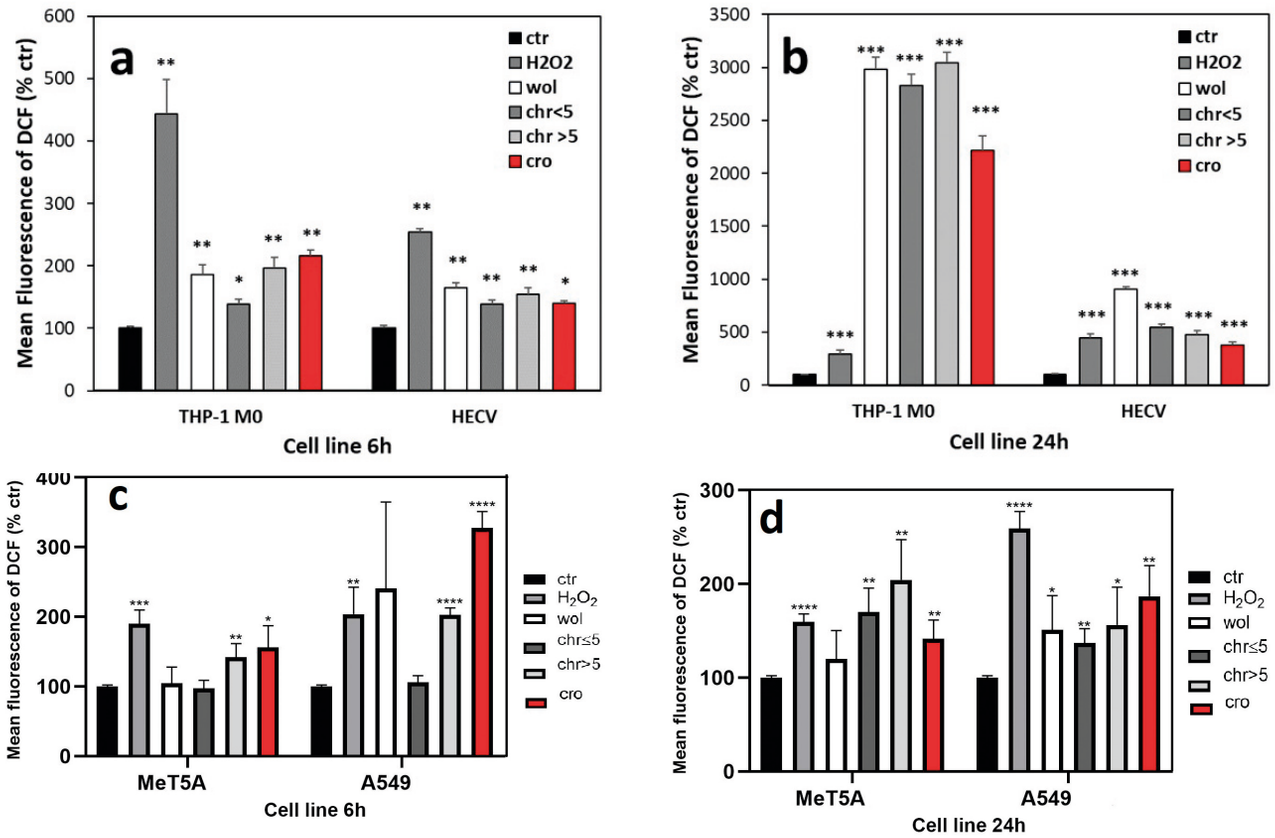

Figure 4. Plots of the results of the DCF fluorescence tests measuring the ROS production at 50 µg/ml fibre concentration. a) THP1 and HECV cells after 6 h. b) THP1 and HECV cells after 24 h. c) Met5A and A549 cells after 6 h. d) Met5A and A549 cells after 24 h. Legend: H2O2=positive control H_2O_2 (grey); ctr= control (black); wol= NYAD G wollastonite (white); chr≤5=Russian short (≤5 mm) chrysotile fibres (dark grey); chr>5=Russian long (>5 mm) chrysotile fibres (light grey); cro=UICC crocidolite (red). Asterisks indicate significance in paired Tukey test as compared to the relative untreated control (*p<0.05; **p<0.005; ***p<0.0005, ****p<0.0001, respectively).

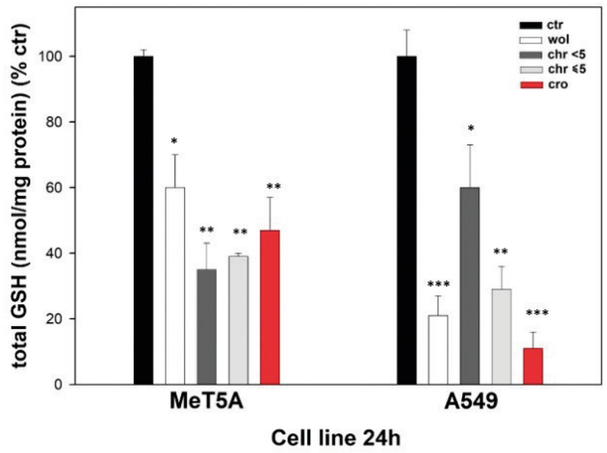

Figure 5. Plot of results of the test measuring the intracellular reduced glutathione fraction (GSH) on Met5A and A549 cells after 24 h. Legend: ctr= control (black); wol= NYAD G wollastonite (white); chr£5=Russian short (≤5 µm) chrysotile fibres (dark grey); chr>5=Russian long (>5 µm) chrysotile fibres (light grey); cro=UICC crocidolite (red). Asterisks indicate significance in paired Tukey test as compared to the relative untreated control (*p<0.05; **p<0.005; ***p<0.0005; respectively).

crocidolite (c), and long chrysotile fibres (d) after 24 h. The presence of free radicals is revealed by the appearance of the typical spectrum of the [DMPO-OH]• adduct characterized by four lines. All the samples catalysed the formation of free radicals, indicating the presence of catalytic reactive sites at the surface of the fibres.

Figure 7 is a summary plot that compares the overall scores of toxicity *in vitro* calculated for the four investigated fibres. The score of each fibre (wol= NYAD G wollastonite; chr≤5=Russian short (≤5 µm) chrysotile fibres; chr>5=Russian long (>5 µm) chrysotile fibres; cro=UICC crocidolite) has been calculated by the mean of the normalized deviations D_i of each value measured in the *in vitro* tests from control values (100%), according to the following equation:

In more detail, the value of the control (100%) is subtracted from each value x_i measured during the *in vitro* tests. Each residual value x_i is then normalized (divided by 100). The mean of all the x_i values is then calculated for the four fibres wol, chr≤5, chr>5, and cro. A few

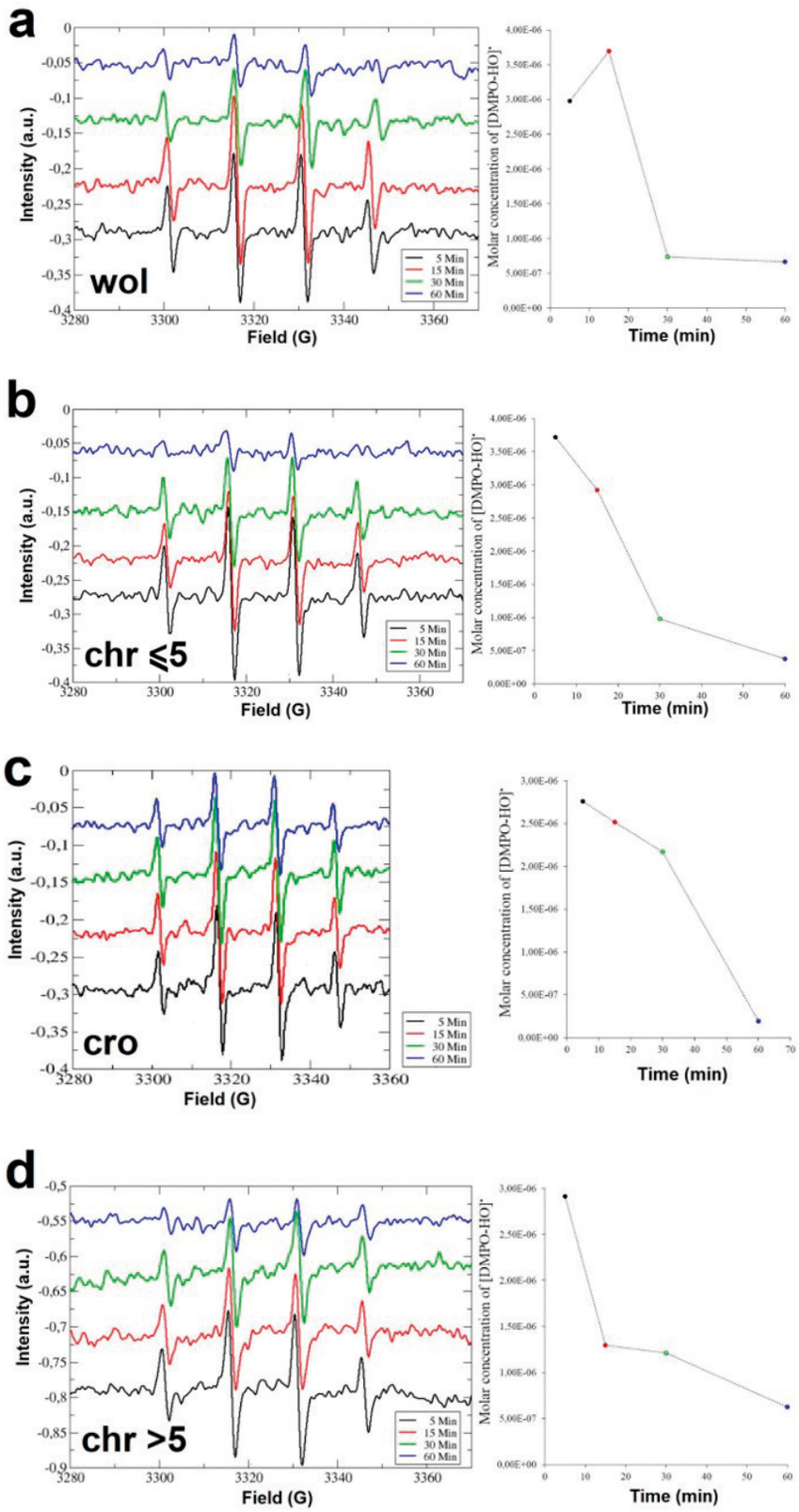

Figure 6. EPR spectra of [DMPO-OH]• adduct and quantitative plot of (A) wol= NYAD G wollastonite; (B) chr≤5=Russian short (≤5 mm) chrysotile fibres; (C) cro=UICC crocidolite; (D) chr>5=Russian long (>5 μm) chrysotile fibres.

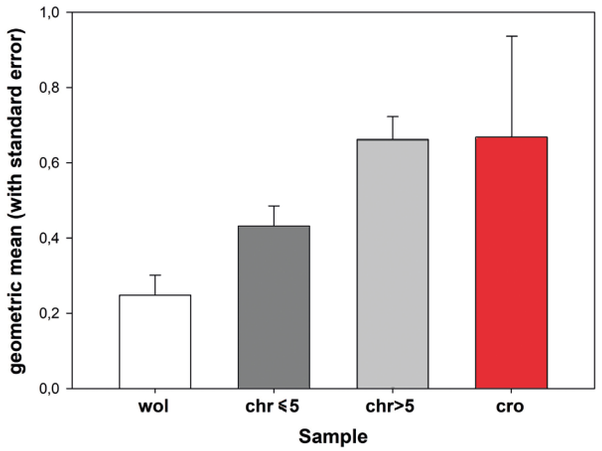

Figure 7. A plot that compares the overall scores of *in vitro* toxicities calculated for the four investigated fibres. Legend: wol= NYAD G wollastonite (white); chr≤5=Russian short (≤5 mm) chrysotile fibres (dark grey); chr>5=Russian long (>5 mm) chrysotile fibres (light grey); cro=UICC crocidolite (red). See text for details.

obvious outliers were removed from the calculation. The variances were also calculated and plotted in Figure 7. The calculation foil printed as PDF file has been provided as Supplementary Material to this article.

Considering that zero is the basic value of the control, the negative carcinogenic standard wollastonite displays the lower score of 0.25(0.05) and the positive carcinogenic standard crocidolite displays the higher score of 0.67(0.28). Russian chrysotile with short fibres has a significantly lower score (0.43(0.05)) with respect to the long fibres [0.66(0.07)]. The latter has a score comparable to that of crocidolite.

The negative standard wollastonite

It may be surprising that wollastonite, despite being used as a negative standard, shows activity *in vitro* that reduces cell viability and/or increases cell mortality (wol white columns in Figure 1 and 3). Wollastonite also catalyses the production of ROS. In all cell cultures (wol white columns in Figure 4), wollastonite produced more ROS than other fibres and control. This finding has already been well described in the literature. Governa et al. (1998) noted that, compared to asbestos, wollastonite produces higher levels of ROS in PMN suspensions. An explanation can be that the larger size of its fibres prevents complete ingestion by phagocytes. The significant difference in ROS generation observed between raw and milled wollastonite fibres and the negative results obtained with surface-modified fibres indicate that a large part of the ROS generated are not free radicals. Governa et al. (1998) and later Maxim and Connell (2005) therefore concluded that, since the toxicity of asbestos is mainly due to the generation of free radicals, the thesis of Nejjari et al. (1993) and Aslam et al. (1995) that wollastonite fibres are less toxic than asbestos fibres is supported. The cytotoxic action of wollastonite does not make it a carcinogenic material. In fact, Di Giuseppe et al. (2021b) reported the results of genotoxicity tests using the g-H2AX assay (Garcia-Canton et al., 2012) on THP1 cells exposed to wollastonite fibres for 24 h and showed that the macrophages challenged with crocidolite UICC displayed a significant high rate of double strand breaks while no significant difference with respect to control was observed in wollastonite NYAD G treatment.

It is important to stress the concept that a cytotoxic action *in vitro* is only a predictive tool for carcinogenicity. Further strong evidence that an agent exhibits key characteristics of carcinogens are required to make it a *probable* or *possible* carcinogen. Outstanding examples of minerals used by man since ancient times that have never posed a hazard to human health, but that show cytotoxic activity, are the layer silicates kaolinite and mica. Regarding kaolinite, Governa et al. (1995) observed a high ROS production with kaolinite, casting doubt on the ability of pathogenic mineral dusts *in vitro* to induce a greater release of ROS than non-pathogenic mineral dusts. Regarding mica, Grytting, et al. (2022) reported that muscovite was the only major rock-forming mineral consistently associated with increased cytotoxicity and cytokine release in their cell models. Said that, regarding wollastonite, the IARC (1997) stated that there is insufficient evidence in both humans and animals to support the carcinogenicity of that agent.

Besides the fact that non-animal *in vitro* toxicity tests are simplified systems attempting to reproducing the complexity of the *in vivo* environment, and that false positive and false negative are frequent in these simplified cell systems, one of the basic biases that must be considered is the so-called "background interference due to inclusion of particles" (Aslantürk, 2018). Any cell culture in contact with "foreign" bodies such as dust particles inevitably suffers a detrimental physical effect compared to the control cell culture alone (ctr black column in our figures) and this effect is regarded as a background interference (Aslantürk, 2018) and must be taken into account to avoid or reduce false positives and false negatives. The reduction in cell viability usually occurs due to physical-mechanical damage of cell membranes in contact with foreign particles (Aslantürk, 2018).

Some degree of toxicity and cell death on in vitro cells lines, as well as a minimal inflammatory response is to be expected whatever mineral is used. Very likely, this is also what happens in vivo since respirable mineral particles or fibres, and dusts in general, once inhaled always cause some irritation and a transitory inflammation in the

lung until the foreign bodies are completely removed. This is just an acute, transitory response that is usually resolved in a matter of days, when the inhaled dusts or mineral particles are not really toxic, like wollastonite. Conversely, in the case of toxic mineral fibres, acute responses may be more intense, or similar to non-toxic fibres, but the difference in this case is the prolonged state of inflammation that they cause, posing the bases to the onset of long-term lung diseases (Perkins, 2012).

For these reasons, the use of a negative standard is of paramount importance to verify the accuracy of the system and avoid the classification of any powder, even the safest (e.g., calcium carbonate), as toxic. Confirmation of the efficacy of this approach for verifying the accuracy of *in vitro* toxicity data using a negative standard consisting of Portland cement is described in Giantomassi et al. (2010). Therefore, it should not be surprising that in cell viability tests wollastonite shows a reduction compared to the control (for example, a 10% reduction compared to ctr is observed in the THP1 M0 MTT 24h test in Figure 1a). The value is further reduced by 17% (83% cell viability) after 48 h (Figure 1b). This effect of reduced cell viability over time is also likely not attributable to the chemical-physical nature of the fibre but physiological, due to an increase in the number of cell membranes that come into physical contact with the dust and become damaged. It should also be noted that during *in vitro* cell viability tests, counting errors are plus or minus 10% (Aslantürk, 2018). Therefore, a value of 90% cannot be considered as significant.

Chrysotile vs crocidolite

Our data show that the positive carcinogenic standard UICC crocidolite (cro red columns in Figure 1a and 1b) has a cytotoxic action at both 24 h and 48 h apparently lower or comparable to that of the chrysotile fibres. Regardless of the length of the fibres, a lower MTT cell viability (or higher mortality in the case of the LDH assay) is observed for chrysotile with respect to the control and the crocidolite fibres, witnessing an acute toxicity potential of both short and long chrysotile fibres. These findings support the model that, although significantly reduced in intensity, short chrysotile fibres also display an *in vitro* cytotoxic potential.

The difference in the intensity of the cytotoxic action of chrysotile vs. crocidolite in the short term (Figure 3) is in line with literature data. The results of COMET (DNA strand breakage) tests revealed that chrysotile has a more intense activity at the same weight concentration than amphibole asbestos (Mossman and Gualtieri, 2020). Furthermore, Craighead et al., (1980) and Mossman et al. (2011) demonstrated that chrysotile is more cytotoxic than crocidolite or amosite at the same mass or fibre concentration in rodent and human lung epithelial and mesothelial cells. The toxicity effects of chrysotile can be partly explained for phagocytic cells by the so-called 'Trojan Horse Effect' (Gualtieri et al., 2019). According to this model, metal nanoparticles when phagocytosed either partially or completely, in contact with acidic phagolysosomes, dissolve and release toxic metal ions into the intracellular or extracellular environment, inducing cyto- and geno-toxic effects (Studer et al., 2010). In the same way as nanoparticles do, this effect could explain the cytotoxicity of chrysotile, which, once engulfed by phagocytic cells, undergoes rapid dissolution upon contact with phagolysosomal acidic fluids. Dissolution of the octahedral sheet of the chrysotile fibres results in a release of metals (especially Fe) with cyto- and geno-toxic action. This occurs to a much lesser extent for biodurable crocidolite, which therefore exerts less acute-phase toxicity.

If we consider the overall toxicity potential of chrysotile vs. crocidolite which takes into account the chronic action of the fibres, it is certainly possible to support the model that chrysotile has a lower toxicity potential with respect to amphibole asbestos. Gualtieri (2018) published FPTI scores of chrysotile samples that are significantly lower than those of amphibole asbestos samples and this difference is basically because chrysotile is not biodurable. Bernstein (2022) stressed this point on the difference in biosolubility between the two mineral types, chrysotile and amphibole asbestos, and that chrysotile inhalation biopersistence studies have shown that even with significant long fibre (>20 μm) exposure, chrysotile breaks down into smaller particles and fibres which are cleared from the lung with half-times of 1 day to 15 days, following a 5-day exposure.

Bernstein (2022) also reported that "amphibole asbestos is encased by a crystalline silica shell which has been shown to have little solubility ... In contrast, chrysotile has been shown to dissociate into individual fibrils at pH 7.4 and to break down into amorphous silica particles at pH 4.5". This sentence is incorrect because: (i) amphiboles are not "encased by a crystalline silica shell". This is an odd representation of the structure of these minerals. (ii) chrysotile does not necessarily dissociate into individual fibrils at pH 7.4. (iii) chrysotile does not necessarily break down into amorphous silica particles at pH 4.5 but, following acid leaching, the amorphous silica relicts can retain their fibrous habit, although with different mechanical and tensile strength (Gualtieri et al., 2019).

Finally, it should be observed that metal release may also explain the primary production of ROS which is abundant in all the mineral fibres observed, including the negative standard wollastonite.

Short chrysotile vs long chrysotile

The results of our *in vitro* experiments evidenced a greater cytotoxic activity of the long chrysotile fibres compared to the short ones. The different behaviour of the short and long chrysotile samples can be interpreted with the inefficiency of the cells to uptake the long fibres. In contact with the long fibres, cells can undergo physical insult and frustrated partial phagocytosis resulting in a significantly higher apoptotic cell death rate. Accordingly, we have seen that, although less evident in absolute terms, even for ROS production, long-fibre chrysotile has a higher activity (160-180%) than short-fibre chrysotile (130-150%) with both THP-1-derived M0 macrophages and HECV cell cultures.

The results of our *in vitro* toxicity study are in line with the literature data (see for example, Kaw et al., 1982; Hesterberg and Barrett, 1984; Riganti et al., 2003) supporting the hypothesis that long chrysotile fibres are more hazardous than short fibres (see the overall toxicity score in Figure 7). Notwithstanding, in agreement with the prediction from the scores of the FPTI model, we have measured *in vitro* toxicity significantly different from the control and standards even from the chrysotile sample batches with fibres ≤5μm. Hence, although the *in vitro* tests are predictive and do not provide direct observation of the pathogenicity potential, we cannot support the model of the "zero hazard" (that is, "short(er) fibres would have any effect and do not contribute to the health effects of asbestos") of short chrysotile fibres (see for example, Davis and Jones, 1988; Roggli, 2015; Barlow et al., 2017; Bernstein, 2022).

The issue of the normalization of the administered dose

An issue concerning the *in vitro* test is the normalization of the administered dose of the fibres to the cell cultures. The use of different administration metrics, in particular the concentration of test substance in terms of mass (as it was done here), number of particles/fibres or specific surface area does not always provide reliable measures of the actual dose of substance administered to target cells. Depending on the nature of the administered particles and their size, this factor may be a major cause of the failure of *in vitro* models in predicting *in vivo* response, as discussed by Hinderliter et al. (2010), Sayes et al. (2006) and Warheit et al. (2009). According to Oberdörster (1994), chrysotile appears to have the same toxicity towards macrophages as amphibole fibres when doses of equal mass are administered. However, based on the number of fibres, which are higher in chrysotile than in amphiboles for the same sample mass, chrysotile appears to be less toxic to macrophages. Hence, apparently the importance of the appropriate dose parameter, i.e., the mass, the number or the surface area of the fibres, should be considered for *in vitro* and *in vivo* studies (Oberdörster 1994). The scenario is still much debated, although fibre concentration and size must be considered when assessing a potential risk (Mossman et al. 1990). Some authors like Governa et al. (1998) normalised the dose of mineral particles with different physical characteristics (size and surface area) to achieve comparable specific surface area. By dosing fibres for the total surface area, Governa et al. (1998) solved the problem of standardising heterogeneous mineral particles and thus obtained comparable responses in short-term *in vitro* experiments. According to Bernstein (2022), normalization with respect to the mass of the samples has the disadvantage of not predicting *a priori* the number of asbestos fibres in contact with the cells with the result of having heterogeneous quantities of fibres among the investigated samples and possibly "abnormal" values in relation to the number of cells in the cultures analysed. Bernstein (2022) reports values of 500,000 ff/cell (Huang, 1979) and 70,000 ff/cell (Jaurand et al., 1981) as examples of disproportionate ratios that may invalidate the results of the *in vitro* experiments. This number of applied fibres per cell is certainly "abnormal" and, according to Bernstein (2022), far exceeds the few fibres per cell occasionally observed following exposure to ca. 250 ff WHO standard (L>5 μm, W<3 μm and L:W>3) per cm^3 of chrysotile (Bernstein et al., 2021). Said that for equal administered mass, a sample of mineral fibre with a larger surface area will obviously bring a higher number of fibres into contact with cells, the statement of Bernstein (2022) "*… few fibers per cell that are occasionally seen following exposure to ~250 WHO fibers/cm^3 of chrysotile*" is misleading because: (i) conditions of professional exposure are not specified. (ii) type of cells is not specified. (iii) the definition of WHO fibres encompasses a wide continuous range of fibre lengths and widths. For example, at equal lengths, a "few" WHO fibres with W=2.9μm, as seen by optical microscopy counting, can be actually 841 single fibres with W=0.1μm.

Below are the reasons to support the significance of the results of our *in vitro* study:

1) we are well aware that some *in vitro* experiments can have a problem of fibre overload with a heterogeneous distribution of fibres suffocating the cells (see an example in the original Figure 8 showing a 100 μg/ml concentration of erionite fibres in contact with THP-1 cells). Here, we have used high density of cells (e.g., 250000 cells/ml in the MTT tests) and the fibre to cell ratio observed in our cell cultures (variable from ca. 1 to 50 ff/cell) are orders of magnitude lower than the 'fibre overload' situations described by Bernstein (2022);

2) chrysotile fibres are inevitably aggregated into bundles and bound by weak van der Waals forces, hydrogen bonding or stronger chemical bonds due to inter-

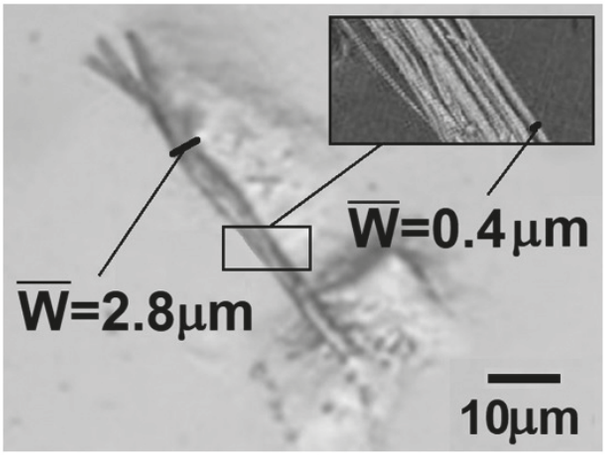

Figure 8. An example of THP1 cell culture with the cells in contact with long chrysotile fibres. The contact occurs between the cells and fibre aggregates/bundles (with mean W=2.8 μm, as observed with optical microscopy) and not (only) between the cells and single fibres (mean W=0.4 μm, as observed with electron microscopy). If, for the normalization of the dose for the *in vitro* tests by fibre number, the number of SEM single fibres is considered, as reported in the literature, the fibre/cell ratio is way much higher than the observed fibre/cell ratio.

grain crystallisation. Aggregation of chrysotile fibres has been observed for almost 50 years with chrysotile fibres that tend to consist of bundles of fibrils often curvilinear with splayed ends (Langer et al., 1974). For this reason, the actual count of fibres per unit mass is much lower and cells *in vivo* mostly interact with these aggregates of fibres and not only with individual fibres or fibrils. In our systems, the actual mean W of the fibres aggregates in the cell cultures at 50 mg/ml observed with optical microscopy is about 2.8 μm for long chrysotile fibres, 1.4 μm for short chrysotile fibres and 2.0 for crocidolite. These values are obviously much greater than the mean W of the fibres observed with SEM (0.4 μm, 0.15 μm and 0.35 μm for long chrysotile, short chrysotile and crocidolite, respectively). Following the ideal picture illustrated in Figure 8 for the long chrysotile fibres in a cell culture, at equal mass, these numbers yield extremely different densities of fibres. In 50 mg, we calculated 5,185,797 long chrysotile fibres (ca. 21 ff/cell), 574,912,232 short chrysotile fibres (ca. 2,300 ff/cell), and 8,627,383 (ca. 35 ff/cell) crocidolite fibres, respectively. The numbers greatly decrease if we consider the observed actual number of fibre aggregates/bundles that get in contact with the cells: in 50 mg, we calculated 207,272 long chrysotile fibres (ca. 1 ff/cell), 12,935,525 short chrysotile fibres (ca. 51 ff/cell), and 343,151 (ca. 1.4 ff/cell) crocidolite fibres, respectively. We observe that a single cell can interact with a single chrysotile fibre or fibril but mostly with an aggregate/bundle of them. Hence, the figures of ca. 1 ff/cell for long chrysotile fibres, ca. 51 ff/cell for short chrysotile fibres, and ca. 1.4 ff/cell for crocidolite fibres should be considered. As an example, Figure 9 shows a THP-1 cell cluster with the long (>5μm) chrysotile fibres at a mass concentration of 100 μg/ml (panel A). The cells, indicated by red dashed lines, attempt to uptake single fibres (a single fibre with W=0.3 μm in panel B) but mostly fibre bundles/aggregates (specifically a fibre bundle with W=3 μm composed of 25 single fibres of mean 0.4 μm width in panel C). The application of a single-fibre vs. single cell interaction model, as is the case of nanoparticles, glass wool/rock fibres (Zeidler-Erdely et al., 2006) to asbestos fibres and especially to chrysotile with a normalisation metrics by fibre number is hence not justified;

3) a proof of the model described at point 2) is that the surface area values of the two chrysotile samples and crocidolite are not very different despite the fact that the theoretical number of fibres per unit mass of the short-fibre chrysotile is way much higher than the others;

4) another proof of the model described at point 2) is the normalization by fibre volume. If we consider normalising by volume, the ratio between the volume occupied by the fibres and the volume occupied by the cells in culture is comparable for the different types of fibres. In fact, assuming an average diameter of about 20 μm for the approximately spherical cells, their volume will be 0.00105 cm^3 for a concentration of 50 μg/ml of fibres and the fibre/cell volume ratio will be 0.0143 for crocidolite and 0.0185 for chrysotile;

5) imposing a normalisation metrics by (single) fibre number (as measured by SEM) may be somehow pretextual as the comparison between chrysotile and positive standard such as crocidolite would inevitably result in very low mass doses of the chrysotile samples. In our case, for the same single-fibre/number of cells ratio of 34.5 calculated for crocidolite at 50 μg/ml, the mass dose of short-fibre chrysotile to be administered to the cells should be 0.75 μg/ml. Obviously, with such 'homeopathic' dose, the toxicity effects of chrysotile would be null as predicted by the model of the 'pro-chrysotile' community (e.g. Bernstein, 2021; 2022), claiming that chrysotile has negligible toxicity potential.

CONCLUSIONS

In this work, we have calculated the fibre potential toxicity/pathogenicity index (FPTI) of Russian commercial chrysotile with long fibres (L>5μm) and short fibres (L≤5μm). The FPTI value of the long-fibre chrysotile (2.35) is greater than that of short-fibre chrysotile (2.18) predicting a greater potential of toxicity/pathogenicity of the former. The FTPI value of short-fibre

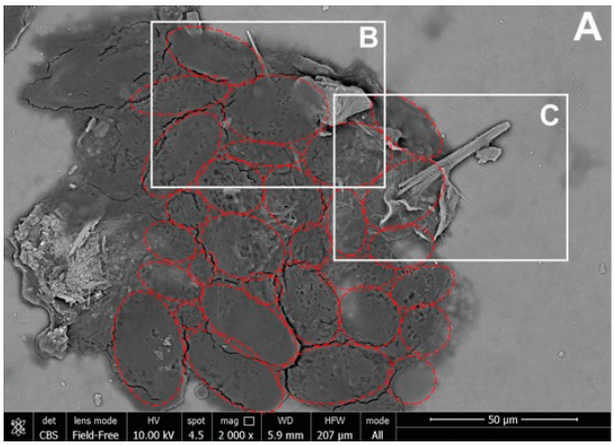

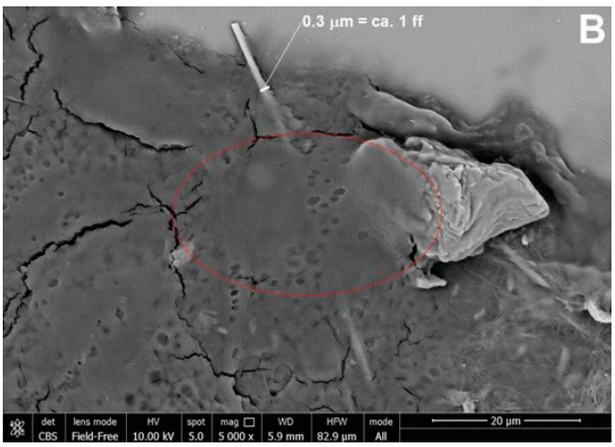

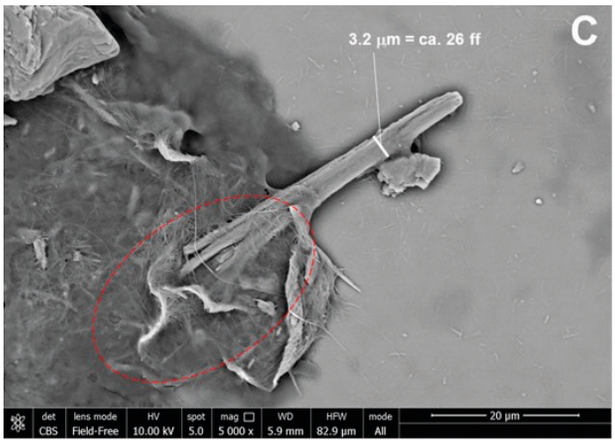

Figure 9. The actual interaction of a THP-1 cell cluster with the long (>5µm) chrysotile fibres in our *in vitro* experiments at a concentration of 100 µg/ml (panel A). The cells attempt to uptake single fibres (specifically a fibre with W=0.3 µm in case B, and the correspondent enlarged panel) but mostly fibre bundles/aggregates (specifically a fibre bundle with W=3 µm composed of 25 single fibres of mean 0.4 µm width in case C, and the correspondent enlarged panel). The red dashed lines indicate the shape of the cells, visible as dark grey rounded bodies.

chrysotile is greater than that of the negative carcinogenic standard NYAD G wollastonite (1.92-2.12) but lower than that of the positive carcinogenic standard UICC crocidolite (2.67). Although the FPTI model is a theoretical tool to predicting the potential toxicity and carcinogenicity of a mineral fibre based on all its crystal-chemical-physical parameters inducing biological adverse effects, the results of the *in vitro* toxicity tests are in line with the prediction. The negative carcinogenic standard wollastonite displays the lower score of 0.25, followed by the short-fibre chrysotile (0.43) and the long-fibre chrysotile (0.66), which higher score is comparable to that of the positive carcinogenic standard crocidolite (0.67) (Figure 7). The *in vitro* toxicity score of chrysotile is comparable to that of crocidolite (Figure 7) because only acute-short terms effects are considered while crocidolite toxicity potential is greater than that of chrysotile when chronic long-term effects are considered, as predicted by the FPTI model.

We cannot share the postulate of Bernstein (2022) claiming that "short asbestos fibres are like innocuous dust" because our results yield the following inequality as far as the toxicity *in vitro* in regarded: wollastonite < Short-fibre chrysotile <l ong-fibre chrysotile ≤ crocidolite. Paraphrasing the sentence of the Agency for Toxic Substances and Disease Registry (2004), we can speculate that "*chrysotile fibres shorter than 5 µm are unlikely but can cause cancer in humans*".

In this work, we have discussed why wollastonite, assumed as negative carcinogenic standard, has biological activity and, although to a lower extent, toxic potential *in vitro*.

We also discussed the conundrum of the normalization metrics for the *in vitro* tests by fibre mass vs fibre number highlighting the pros and cons of the different approaches, with a special attention to the limits in the prediction of the carcinogenicity of mineral fibres.

ACKNOWLEDGEMENTS

This research was conducted within the research project *"Fibres, A Multidisciplinary Mineralogical, Crystal-Chemical and Biological Project to Amend the Paradigm of Toxicity and Cancerogenicity of Mineral Fibres"* (Code PRIN20173X8WA4).

This paper is dedicated to Alessandro Guastoni who prematurely passed away on December 7th, 2022, at the age of 56, for a tragic casualty during an expedition in search of new minerals.

REFERENCES

ANSES, 2015. Effets sanitaires et identification des fragments de clivage d'amphiboles issus des matériaux de carrière:

Rapport d'expertise collective, 218 pp.

ANSES, 2017. Particules minérales allongées. Identification des sources d'émission et proposition de protocoles de caractérisation et de mesures: Rapport d'expertise collective, 184 pp.

Aslam M., Arif M.J., Rahman O., 1995. Red blood cell damage by wollastonite: In vitro study. Journal of Applied Toxicology 15, 27-31.

Aslantürk Ö.S., 2018. In vitro cytotoxicity and cell viability assays: principles, advantages, and disadvantages. Genotoxicity-A predictable risk to our actual world 2, 64-80.

ATSDR, 2004. Toxicological profile for synthetic vitreous fibers additional resources. Public Health Service Agency for Toxic Substances. http://www.atsdr.cdc.gov/toxprofiles/tp161.html.

Ballirano P., Bloise A., Gualtieri A.F., Lezzerini M., Pacella A., Perchiazzi N., Doga M., Dogan A.U., 2017. Crystal habit of mineral fibres. In A.F. Gualtieri, Ed., Mineral Fibres: Crystal Chemistry, Chemical-Physical Properties, Biological Interaction and Toxicity. EMU Notes in Mineralogy, European Mineralogical Union, London 18, 11-53.

Barlow C.A., Grespin M., Best E.A., 2017. Asbestos fiber length and its relation to disease risk. Inhalation Toxicology 29, 541-554.

Baronnet A. and Devouard B., 1996. Topology and crystal growth of natural chrysotile and polygonal serpentine. Journal of Crystal Growth 166, 952-960.

Bernstein D.M., 2022. The health effects of short fiber chrysotile and amphibole asbestos. Critical Reviews in Toxicology 52, 89-112.

Bernstein D.M., Dunnigan J., Hesterberg T., Brown R., Velasco J.A.L., Barrera R., Hoskins J., Gibbs A., 2013. Health risk of chrysotile revisited. Critical Reviews in Toxicology 43, 154-183.

Bernstein D.M., Toth B., Rogers R.A., Kunzendorf P., Phillips J.I., Schaudien D., 2021. Final results from a 90-day quantitative inhalation toxicology study evaluating the dose-response and fate in the lung and pleura of chrysotile-containing brake dust compared to TiO_2, chrysotile, crocidolite or amosite asbestos: Histopathological examination, confocal microscopy and collagen quantification of the lung and pleural cavity, Toxicology and Applied Pharmacology 424, 1-20.

Bey E. and Harington J.S., 1971. Cytotoxic effects of some mineral dusts on Syrian hamster peritoneal macrophages. Journal of Experimental Medicine 133, 1149-1169.

Boulanger G., Andujar P., Pairon J.C., Billon-Galland M.A., Dion C., Dumortier P., Brochard P., Sobaszek A., Bartsch P., Paris C., Jaurand M.C., 2014. Quantification of short and long asbestos fibers to assess asbestos exposure: a review of fiber size toxicity. Environmental Health 13, 1-18.

Buettner G.R., 1987. Spin trapping: ESR parameters of spin adducts. Free Radical Biology and Medicine 3, 259-303.

Ciapetti G., Cenni E., Pratelli L., Pizzoferrato A., 1993. In vitro evaluation of cell/biomaterial interaction by MTT assay. Biomaterials 14, 359-364.

Circu M.L. and Aw T.Y., 2008. Glutathione and apoptosis. Free Radical Research 42, 689-706.

Craighead J.E., Mossman B.T., Ezerman E.B., Adler K.B., 1980. Isolation and spontaneous trans-formation of hamster tracheal epithelial cells. Cancer Research 40, 4403-4409.

Davis J.M. and Jones A.D., 1988. Comparisons of the pathogenicity of long and short fibres of chrysotile asbestos in rats. British Journal of Experimental Pathology 69, 717-737.

Di Giuseppe D., Zoboli A., Nodari L., Pasquali L., Sala O., Ballirano P., Malferrari D., Raneri S., Hanuskova M., Gualtieri A.F., 2021a. Characterization and assessment of the potential toxicity/pathogenicity of Russian commercial chrysotile. American Mineralogist 106, 1606-1621.

Di Giuseppe D., Scognamiglio V., Malferrari D., Nodari L., Pasquali L., Lassinantti Gualtieri M., Scarfì S., Mirata S., Tessari U., Hanuskova M., Gualtieri A.F., 2021b. Characterization of Fibrous Wollastonite NYAD G in View of Its Use as Negative Standard for In Vitro Toxicity Tests. Minerals 11, 1378.

Dodson R.F., Atkinson M.A., Levin J.L., 2003. Asbestos fiber length as related to potential pathogenicity: a critical review. American Journal of Industrial Medicine 44, 291-297.

Egilman D., 2009. Fiber types, asbestos potency, and environmental causation: a peer review of published work and legal and regulatory scientific testimony. International journal of occupational and environmental health 15, 202-228.

Garcia-Canton C., Anadón A., Meredith C., 2012. H2AX as a novel endpoint to detect DNA damage: Applications for the assessment of the in vitro genotoxicity of cigarette smoke. Toxicology in Vitro 26, 1075-1086.

Giantommasi F., Gualtieri A.F., Santarelli L., Tomasetti M., Lusvardi G., Lucarini G., Governa M., Pugnaloni A., 2010. Biological effects and comparative cytotoxicity of thermal transformed asbestos-containing materials in a human alveolar epithelial cell line. Toxicology in vitro 24, 1521-1531.

Goodglick L.A. and Kane A.B., 1990. Cytotoxicity of long and short crocidolite asbestos fibers in vitro and in vivo. Cancer research 50, 5153-5163.

Governa M., Camilucci L., Amati M., Visonà I., Valentino M., Botta G., Campopiano A., Fanizza C., 1998. Wollastonite Fibers in Vitro Generate Reactive Oxygen Species Able to Lyse Erythrocytes and Activate the Complement Alternate Pathway. Toxicological Sciences 44, 32-38.

Governa M., Camilucci L., Amati M., Visonà I., Valentino M., Botta G.C., Campopiano A., Fanizza C., 1998. Wollastonite Fibers in Vitro Generate Reactive Oxygen Species Able to Lyse Erythrocytes and Activate the Complement Alternate Pathway. Toxicological Sciences 44, 32-38.

Governa M., Valentino M., Visona I., Monaco F., Amati M., Scancarello G., Scansetti G., 1995. In vitro biological effects of clay minerals advised as substitutes for asbestos. Cell biology and toxicology 11, 237-249.

Grytting V.S., Refsnes M., Låg M., Erichsen E., Røhr T.S., Snilsberg B., White R.A., Øvrevik J., 2022. The importance of mineralogical composition for the cytotoxic and pro-inflammatory effects of mineral dust. Particle and Fibre Toxicology 19, 1-22.

Gualtieri A.F., 2012. Mineral fibre-based building materials and their health hazards. In F. Pacheco-Torgal, S. Jalali, and A. Fucic, Eds., Toxicity of Building Materials. Woodhead, Cambridge, U.K., 166-195.

Gualtieri A.F., 2018. Towards a quantitative model to predict the toxicity/pathogenicity potential of mineral fibers. Toxicology and Applied Pharmacology 361, 89-98.

Gualtieri A.F., Lusvardi G., Pedone A., Di Giuseppe D., Zoboli A., Mucci A., Zambon A., Filaferro M., Vitale G., Benassi M., Avallone R., Pasquali L., Lassinantti Gualtieri M., 2019. Structure Model and Toxicity of the Product of Biodissolution of Chrysotile Asbestos in the Lungs. Chemical Research in Toxicology 32, 2063-2077.

Gualtieri A.F., 2023. Journey to the Centre of the Lung. The Perspective of a Mineralogist on the Carcinogenic Effects of Mineral Fibres in the Lungs. Journal of Hazardous Materials 442, 130077.

Gualtieri A.F., Mossman B.T., Roggli V.L., 2017. Towards a general model for predicting the toxicity and pathogenicity of minerals fibres. In A.F. Gualtieri, Ed., Mineral Fibres: Crystal chemistry, chemical-physical properties, biological interaction and toxicity. EMU Notes in Mineralogy, European Mineralogical Union, London 18, 501-526.

Gualtieri A.F., Pollastri S., Bursi Gandolfi N., Lassinantti Gualtieri M., 2018. In vitro acellular dissolution of mineral fibres: a comparative study. Scientific Reports 8, 87071.

Hesterberg T.W. and Barrett J.C., 1984. Dependence of asbestos- and mineral dust-induced transformation of mammalian cells in culture on fiber dimension. Cancer Research 44, 2170-2180.

Hinderliter P.M., Minard K.R., Orr G., Chrisler W.B., Thrall B.D., Pounds J.G., Teeguarden J.G., 2010. ISDD: A computational model of particle sedimentation, diffusion and target cell dosimetry for in vitro toxicity studies. Particle and fibre toxicology 7, 1-20.

Huang S.L., 1979. Amosite, chrysotile and crocidolite asbestos are mutagenic in Chinese hamster lung cells. Mutation Research/Genetic Toxicology 68, 265-274.

International Agency for Research on Cancer, 1997. Wollastonite. In IARC Monographs; International Agency for Research on Cancer: Lyon Cedex, France 68, 283-306.

International Agency for Research on Cancer, 2012. Asbestos (chrysotile, amosite, crocidolite, tremolite, actinolite, and anthophyllite). IARC Monography on the Evaluation of Carcinogenic Risks for Human 100C, 219-309.

Janzen E.G., 1971. Spin trapping. Accounts of Chemical Research 4, 31-40.

Jaurand M.C., Magne L., Boulmier J.L., Bignon J., 1981. In vitro reactivity of alveolar macrophages and red blood cells with asbestos fibres treated with oxalic acid, sulfur dioxide and benzo-3, 4-pyrene. Toxicology 21, 323-342.

Kaw J.L., Tilkes F., Beck E.G., 1982. Reaction of cells cultured in vitro to different asbestos dusts of equal surface area but different fibre length. British Journal of Experimental Pathology 63, 109-115.

Korchevskiy A.A. and Wylie A.G., 2022. Dimensional characteristics of the major types of amphibole mineral particles and the implications for carcinogenic risk assessment. Inhalation Toxicology 34, 24-38.

Langer A.M., Mackler A.D., Pooley F.D., 1974. Electron Microscopical Investigation of Asbestos Fibers. Environmental health perspectives 9, 63-80.

LeBouffant L., 1974. Investigation and analysis of asbestos fibers and accompanying minerals in biological materials. Environ Health Perspectives 9, 149-53.

Maxime L.D. and McConnell E.E., 2005. A Review of the Toxicology and Epidemiology of Wollastonite. Inhalation Toxicology 17, 451-466.

Mirata S., Almonti V., Di Giuseppe D., Fornasini L., Raneri S., Vernazza S., Bersani D., Gualtieri A.F., Bassi A.M., Scarfì, S., 2022. The Acute Toxicity of Mineral Fibres: A Systematic In Vitro Study Using Different THP-1 Macrophage Phenotypes. International journal of molecular sciences 23, 2840.

Mossman B.T. and Sesko A.M., 1990. In vitro assays to predict the pathogenicity of mineral fibers. Toxicology 60, 53-61.

Mossman B.T., Lippmann M., Hesterberg T.W., Kelsey K.T., Barchowsky A., Bonner J.C., 2011. Pulmonary endpoints (lung carcinomas and asbestosis) following inhalation exposure to asbestos. Journal of Toxicology and Environmental Health, Part B 14, 76-121.

Mossman B.T. and Gualtieri A.F., 2020. Lung cancer: Mechanisms of carcinogenesis by asbestos. In: Occupational cancers. Springer, Champion 239-256.

Nejjari J., 1993. Mineral fibres: Correlation between oxidising surface activity and DNA base hydroxylation. British Journal of Industrial Medicine 50, 501-504.

Oberdörster G., 1994. Macrophage-associated responses to chrysotile. The Annals of occupational hygiene, 38, 601-615.

Pauling L., 1930. The structure of the chlorites. Proceedings of the National Academy of Sciences USA 16, 578-582.

Perkins T.N., Shukla A., Peeters P.M., Steinbacher J.L., Landry C.C., Lathrop S.A., Steele C., Reynaert N.L., Wouters E.F., Mossman B.T., 2012. Differences in gene expression and cytokine production by crystalline vs. amorphous silica in human lung epithelial cells. Particle and Fibre Toxicology 9, 6.

Ramazzini Collegium, 1999. Call for an international ban on asbestos. Journal of Occupational and Environmental Medicine 41, 830-832.

Riganti C., Aldieri E., Bergandi L., Tomatis M., Fenoglio I., Costamagna C., Fubini B., Bosia A., Ghigo D., 2003. Long and short fiber amosite asbestos alters at a different extent the

redox metabolism in human lung epithelial cells. Toxicology and applied pharmacology 193(1), 106-115.

Sayes C.M., Wahi R., Kurian P.A., Liu Y., West J.L., Ausman K.D., Warheit D.B., Colvin V.L., 2006. Correlating nanoscale titania structure with toxicity: a cytotoxicity and inflammatory response study with human dermal fibroblasts and human lung epithelial cells. Toxicology Science 92, 174-185.

Scognamiglio V., Di Giuseppe D., Lassinantti Gualtieri M., Tomassetti L., Gualtieri A.F., 2021. A systematic study of the cryogenic milling of chrysotile asbestos. Applied Sciences 11, 4826.

Stanton M.F., Layard M., Tegeris A., Miller E., May M., Morgan E., Smith A., 1981. Relation of particle dimension to Carcinogenicity in amphibole asbestos and other fibrous minerals. Journal National Cancer Institute 67, 965-975.

Stipa P., 2021. Recent contributions of EPR to nitrone and nitroxide chemistry. Electron Paramagnetic Resonance 27, 109-145.

Studer A.M., Limbach L.K., Van Duc L., Krumeich F., Athanassiou E.K., Gerber L.C., Moch H., Stark W.J., 2010. Nanoparticle cytotoxicity depends on intracellular solubility: comparison of stabilized copper metal and degradable copper oxide nanoparticles. Toxicology letters 197, 169-174.

Warheit D.B., Sayes C.M., Reed, K.L., 2009. Nanoscale and fine zinc oxide particles: can in vitro assays accurately forecast lung hazards following inhalation exposures? Environmental science & technology 43, 7939-7945.

Yeager H. Jr., Russo D.A., Yañez M., Gerardi D., Nolan R.P., Kagan E., Langer A.M., 1983. Cytotoxicity of a short-fiber chrysotile asbestos for human alveolar macrophages: preliminary observations. Environmental Research 30, 224-232.

Zeidler - Erdely P.C., Calhoun W.J., Ameredes B.T., Clark M.P., Deye G.J., Baron P., Jones W., Blake T., Castranova V., 2006. In vitro cytotoxicity of Manville Code 100 glass fibers: Effect of fiber length on human alveolar macrophages, Particle and Fibre Toxicology 3, 1-7.